

Effects of Temperature Dependent Thermal Conductivity on Magnetohydrodynamic (MHD) Free Convection Flow along a Vertical Flat Plate with Heat Conduction

M. M. Rahman¹, A. A. Mamun², M. A. Azim³, M. A. Alim⁴

¹Dhaka International University, Dhaka-1213, Bangladesh
mrrahmandiu@yahoo.com

²Institute of Natural Sciences, United International University, Dhaka-1209, Bangladesh
mamun3213ssh@gmail.com

³School of Business studies, Southeast University, Dhaka-1213, Bangladesh

⁴Department of Mathematics, Bangladesh University of Engineering and Technology
Dhaka-1000, Bangladesh

Received: 08.10.2007 **Revised:** 29.05.2008 **Published online:** 28.11.2008

Abstract. MHD natural convection flow of an electrically conducting fluid along a vertical flat plate with temperature dependent thermal conductivity and conduction effects is analyzed. The governing equations with associated boundary conditions for this phenomenon are converted to dimensionless forms using a suitable transformation. The transformed non-linear equations are then solved using the implicit finite difference method with Keller-box scheme. Numerical results of the velocity, temperature, skin friction coefficient and surface temperature for different values of the magnetic parameter, thermal conductivity variation parameter, Prandtl number and conjugate conduction parameter are presented graphically. Detailed discussion is given for the effects of the aforementioned parameters.

Keywords: magnetohydrodynamic, free convection, thermal conductivity variation, conduction, finite difference method.

Nomenclature

b	plate thickness	M	magnetic parameter
C_{fx}	local skin friction coefficient	n	thermal conductivity variation parameter
c_p	specific heat at constant pressure	p	conjugate conduction parameter
f	dimensionless stream function	Pr	Prandtl number
g	acceleration due to gravity	T_b	temperature at outside surface of the plate
h	dimensionless temperature	T_f	temperature of the fluid
κ_f, κ_s	fluid and solid thermal conductivities, respectively	T_∞	fluid asymptotic temperature
l	length of the plate		

\bar{u}, \bar{v}	velocity components	η	dimensionless similarity variable
u, v	dimensionless velocity components	τ_w	shearing stress
\bar{x}, \bar{y}	Cartesian coordinates	μ, ν	dynamic and kinematic viscosities, respectively
x, y	dimensionless Cartesian coordinates	ρ	density of the fluid
β	co-efficient of thermal expansion	ψ	dimensionless stream function
θ	dimensionless temperature		

1 Introduction

Flow of electrically conducting fluid in presence of transverse magnetic field is important from the technical point of view and such types of problems have received much attention by many researchers. Experimental and theoretical works on MHD free and forced convection flows have been done extensively but a few investigations were done on the conjugate effects of convection and conduction problems. On the otherhand, the conduction within and convection along (conjugate heat transfer) the plate have a significant importance in many practical problems such as in ablation or perspiration cooling problems as well as in the heterogeneous chemical reaction situations. In these case the information on the interfacial temperature and concentration distribution is essential because the transfer characteristics are mainly determined by the temperature and concentration differences between the bulk flow and the interface. Cheng Long Chang [1] analyzed the conjugate heat transfer of a micropolar fluid for a vertical flat plate. The same problem over a vertical surface in absence of micropolar fluid was studied by Merkin and Pop [2] and Pozzi and Lupo [3]. On the other hand, the axial heat conduction effect in a vertical flat plate over a free convection was studied Miamoto et al. [4]. Pop et al. [5] then extended the analysis to conjugate mixed convection on a vertical surface in porous medium. Moreover, the thermal interaction between laminar film condensation and forced convection along a conducting wall was investigated by Chen Chang [6]. Shu and Pop [7] analyzed the thermal interaction between free convection and forced convection along a vertical conducting wall. Hossain [8] studied the effect of viscous and Joule heating on the flow of an electrically conducting fluid past a semi infinite plate of which temperature varies linearly with the distance from the leading edge and in the presence of uniformly transverse magnetic field. In his paper, using Keller box [9] scheme the equations governing the flow were solved and the numerical solutions were obtained for small Prandtl numbers, appropriate for coolant liquid metal, in the presence of a large magnetic field. Moreover, laminar free convection flow from an isothermal sphere immersed in a fluid with thermal conductivity proportional to linear function of temperature has been studied by Molla et al. [10].

This article describes the effect of magnetic field and temperature dependent thermal conductivity on the coupling of convection flow along and conduction inside a vertical flat plate. The governing boundary layer equations are transformed into a non dimensional form and the resulting non linear system of partial differential equations are solved numerically using the implicit finite difference method together with the Keller box technique [9, 11]. The velocity profiles, temperature distributions, skin friction coefficient as well

as surface temperature distributions are presented graphically. In the following section detailed derivations of the governing equations for the flow and heat transfer and the method of solutions along with the results and discussions are presented.

2 Mathematical analysis

Let us consider a steady laminar natural convection flow of viscous, incompressible and electrically conducting fluid having temperature dependent thermal conductivity along a vertical flat plate of length l and thickness b (Fig. 1). It is assumed that the temperature at the outside surface of the plate is maintained at a constant temperature T_b , where $T_b > T_\infty$, the ambient temperature of the fluid. A uniform magnetic field of strength H_0 is imposed along the \bar{y} -axis.

The governing equations of such flow under the usual boundary layer and the Boussinesq approximations can be written as

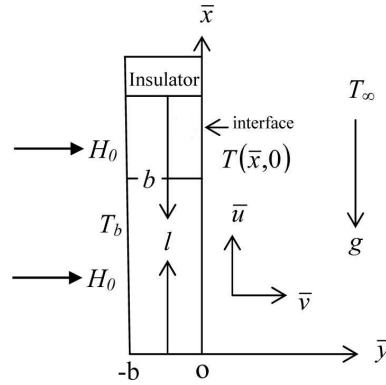


Fig. 1. Physical model and coordinate system

$$\frac{\partial \bar{u}}{\partial \bar{x}} + \frac{\partial \bar{v}}{\partial \bar{y}} = 0, \quad (1)$$

$$\bar{u} \frac{\partial \bar{u}}{\partial \bar{x}} + \bar{v} \frac{\partial \bar{u}}{\partial \bar{y}} = \nu \frac{\partial^2 \bar{u}}{\partial \bar{y}^2} + g\beta(T_f - T_\infty) - \frac{\sigma H_0^2 \bar{u}}{\rho}, \quad (2)$$

$$\bar{u} \frac{\partial T_f}{\partial \bar{x}} + \bar{v} \frac{\partial T_f}{\partial \bar{y}} = \frac{1}{\rho c_p} \frac{\partial}{\partial \bar{y}} \left(\kappa_f \frac{\partial T_f}{\partial \bar{y}} \right). \quad (3)$$

Here we will consider the form of the temperature dependent thermal conductivity which is proposed by Charraudeau [12], as follows

$$\kappa_f = \kappa_\infty [1 + \delta(T_f - T_\infty)] \quad (4)$$

where κ_∞ is the thermal conductivity of the ambient fluid and δ is a constant.

These governing equations have to be solved along with the following boundary conditions [1, 13–15]

$$\left. \begin{aligned} \bar{u} = 0, \quad \bar{v} = 0, \\ T_f = T(\bar{x}, 0), \quad \frac{\partial T_f}{\partial \bar{y}} = \frac{k_s}{bk_f}(T_f - T_b) \end{aligned} \right\} \text{ on } \bar{y} = 0, \bar{x} > 0, \quad (5)$$

$$\bar{u} \rightarrow 0, \quad T_f \rightarrow T_\infty \quad \text{as } \bar{y} \rightarrow \infty, \bar{x} > 0.$$

The non-dimensional governing equations and boundary conditions can be obtained from equations (1)–(5) using the following non-dimensional quantities:

$$\begin{aligned} x = \frac{\bar{x}}{l}, \quad y = \frac{\bar{y}}{l}Gr^{1/4}, \quad u = \frac{\bar{u}l}{\nu}Gr^{-1/2}, \quad v = \frac{\bar{v}l}{\nu}Gr^{-1/4}, \\ \theta = \frac{T_f - T_\infty}{T_b - T_\infty}, \quad Gr = \frac{g\beta l^3(T_b - T_\infty)}{\nu^2}, \end{aligned} \quad (6)$$

where l is the length of the plate, Gr is the Grashof number, θ is the non-dimensional temperature.

Substituting the relations (6) into the equation (1) to (3), we get the following non dimensional equations.

$$\frac{\partial u}{\partial x} + \frac{\partial v}{\partial y} = 0, \quad (7)$$

$$u \frac{\partial u}{\partial x} + v \frac{\partial u}{\partial y} + Mu = \frac{\partial^2 u}{\partial y^2} + \theta, \quad (8)$$

$$u \frac{\partial \theta}{\partial x} + v \frac{\partial \theta}{\partial y} = \frac{1}{Pr}(1 + n\theta) \frac{\partial^2 \theta}{\partial y^2} + \frac{n}{Pr} \left(\frac{\partial \theta}{\partial y} \right)^2, \quad (9)$$

where $Pr = \frac{\mu c_p}{\kappa_\infty}$ is the Prandtl number, $M = \frac{\sigma H_0^2 l^2}{\mu Gr^{1/2}}$ is the magnetic parameter, $n = \delta(T_b - T_\infty)$ is the thermal conductivity variation parameter.

The corresponding boundary conditions (5) then take the following form

$$\begin{aligned} u = 0, \quad v = 0, \quad \theta - 1 = (1 + n\theta)p \frac{\partial \theta}{\partial y} \quad \text{on } y = 0, \quad x > 0, \\ u \rightarrow 0, \quad \theta \rightarrow 0 \quad \text{as } y \rightarrow \infty, \quad x > 0, \end{aligned} \quad (10)$$

where $p = \left(\frac{\kappa_\infty b}{\kappa_s l}\right)Gr^{1/4}$ is the conjugate conduction parameter. The present problem is governed by the magnitude of p as magnetic parameter and thermal conductivity variation parameter. This coupling parameter plays an important role to determine the significance of the wall conduction resistance within the wall.

To solve the equations (8) and (9) subject to the boundary conditions (10), the following transformations are introduced:

$$\begin{aligned} \psi = x^{4/5}(1+x)^{-1/20} f(x, \eta), \\ \eta = y x^{-1/5}(1+x)^{-1/20}, \\ \theta = x^{1/5}(1+x)^{-1/5} h(x, \eta). \end{aligned} \quad (11)$$

here η is the similarity variable and ψ is the non-dimensional stream function which satisfies the equation of continuity and is related to the velocity components in the usual way as $u = \partial\psi/\partial y$ and $v = -\partial\psi/\partial x$. Moreover, $h(x, \eta)$ represents the dimensionless temperature. Thus we get

$$\begin{aligned} f''' + \frac{16+15x}{20(1+x)}ff'' - \frac{6+5x}{10(1+x)}f'^2 - Mx^{2/5}(1+x)^{1/10}f' + h \\ = x \left(f' \frac{\partial f'}{\partial x} - f'' \frac{\partial f}{\partial x} \right), \end{aligned} \quad (12)$$

$$\begin{aligned} \frac{1}{Pr}h'' + \frac{n}{Pr} \left(\frac{x}{1+x} \right)^{1/5} hh'' + \frac{n}{Pr} \left(\frac{x}{1+x} \right)^{1/5} h'^2 + \frac{16+15x}{20(1+x)}fh' - \frac{1}{5(1+x)}f'h \\ = x \left(f' \frac{\partial h}{\partial x} - h' \frac{\partial f}{\partial x} \right), \end{aligned} \quad (13)$$

where prime denotes partial differentiation with respect to η . The boundary conditions as mentioned in equation (10) then take the following form:

$$\begin{aligned} f(x, 0) = f'(x, 0) = 0, \\ [(1+x)^{-1/4} + nx^{1/5}(1+x)^{-9/20}h(x, 0)]ph'(x, 0) = \left(\frac{x}{1+x} \right)^{1/5} h(x, 0) - 1, \quad (14) \\ f'(x, \infty) \rightarrow 0, \quad h(x, \infty) \rightarrow 0. \end{aligned}$$

The set of equations (12) and (13) together with the boundary conditions (14) are solved numerically by applying implicit finite difference method with Keller box [9] scheme. Since a good description of this method and its application to the boundary layer flow problems are given in the book by Cebeci and Bradshaw [11], the details of the method have not been presented in this paper. From the process of numerical computation, in practical point of view, it is important to calculate the values of the surface shear stress in terms of the skin friction coefficient. This can be written in the non-dimensional form as

$$C_f = \frac{Gr^{-3/4}l^2}{\mu\nu}\tau_w, \quad (15)$$

where τ_w ($\tau_w = \mu(\partial\bar{u}/\partial\bar{y})_{\bar{y}=0}$) is the shearing stress. Using the new variables described in (6), the local skin friction co-efficient can be written as

$$C_{fx} = x^{2/5}(1+x)^{-3/20}f''(x, 0). \quad (16)$$

The numerical values of the surface temperature are obtained from the relation

$$\theta(x, 0) = x^{1/5}(1+x)^{-1/5}h(x, 0). \quad (17)$$

We have also discussed the velocity profiles and the temperature distributions for different values of the magnetic parameter, thermal conductivity variation parameter, Prandtl number and conjugate conduction parameter.

3 Results

The main objective of the present work is to analyze the effect of thermal conductivity variation due to temperature on MHD free convection flow along a vertical flat plate in presence of heat conduction. In the simulation the values of the Prandtl number are considered to be 0.733, 1.73, 2.97 and 4.24 that correspond to air, water, methyl chloride and sulfur dioxide, respectively.

The velocity and the temperature fields obtained from the solutions of the equations (12) and (13) are depicted in Fig. 2 to 5. The magnetic field acting along the horizontal direction retards the fluid velocity as shown in Fig. 2(a). From Fig. 2(b), it can be observed that the temperature within the boundary layer increases for the increasing M . The magnetic field decreases the temperature gradient at the wall and increases the temperature in the flow region. It is also observed that the temperature at the interface varies due to the conduction within the plate.

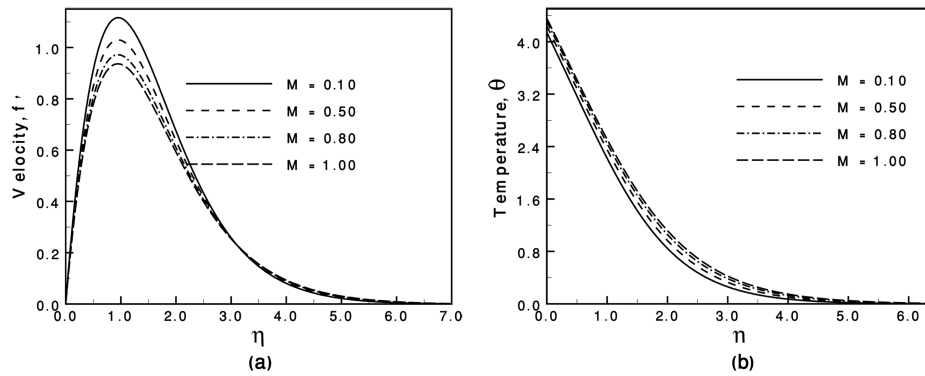


Fig. 2. (a) Variation of velocity profiles and (b) variation of temperature profiles against η for varying of M with $n = 0.01$, $Pr = 0.733$ and $p = 0.25$.

The effect of thermal conductivity variation parameter on the velocity and temperature within the boundary layer with $M = 0.10$, $Pr = 0.733$ and $p = 0.25$ are shown in Fig. 3(a) and Fig. 3(b), respectively. It is seen from Fig. 3(a) and Fig. 3(b) that the velocity and temperature increase within the boundary layer with the increasing value of n . It means that the velocity boundary layer and the thermal boundary layer thickness increase for large values of n . Moreover, the maximum values of the velocity are 1.1166, 1.1466, 1.1768 and 1.2073 for $n = 0.01, 0.03, 0.05$ and 0.07 , respectively and each of which occurs at $\eta = 0.9423$. It is observed that the velocity increases by 7.513 % when n increases from 0.01 to 0.07. Furthermore, the maximum values of the temperature are 4.1430, 4.2533, 4.3632 and 4.4725 for $n = 0.01, 0.03, 0.05$ and 0.07 , respectively and each of which occurs at the surface. It is observed that the temperature increases by 2.593 % when n increases from 0.01 to 0.07.

Fig. 4(a) and Fig. 4(b) illustrate the velocity and temperature profiles for different

values of Prandtl number Pr with $M = 0.10$, $n = 0.01$ and $p = 0.25$. From Fig. 4(a), it can be observed that the velocity decreases as well as the position of the peak velocity moves toward the interface with the increasing Pr . From Fig. 4(b), it is seen that the temperature profiles shift downward with the increasing Pr . It is also observed that the maximum values of the velocity are 1.1184, 0.7830, 0.6187 and 0.5274 for $Pr = 0.733, 1.73, 2.97$ and 4.24 , respectively which occurs at $\eta = 0.9423, 0.8881, 0.8353$ and 0.8353 , respectively. It is seen that the velocity decreases by 52.843 % when Pr increases from 0.733 to 4.24. Furthermore, the maximum values of the temperature are observed to be 4.1464, 3.5023, 3.1633 and 2.9645 for $Pr = 0.733, 1.73, 2.97$ and 4.24 , respectively and each of which occurs at the surface. It is shown that the temperature decreases by 6.285 % when Pr increases from 0.733 to 4.24.

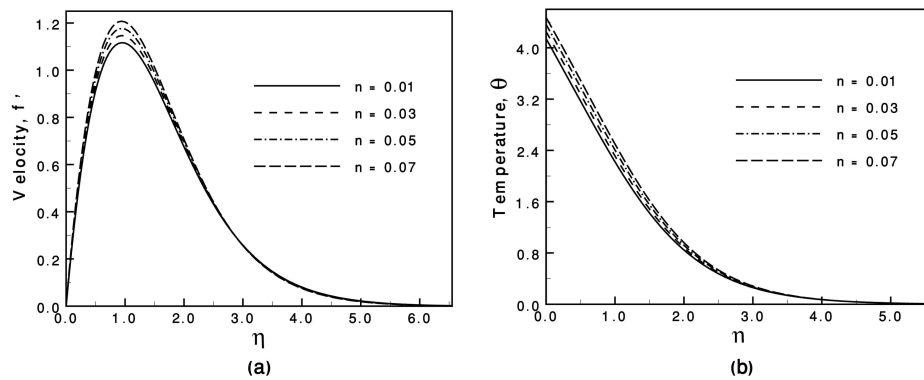


Fig. 3. (a) Variation of velocity profiles and (b) variation of temperature profiles against η for varying of n with $M = 0.10$, $Pr = 0.733$ and $p = 0.25$.

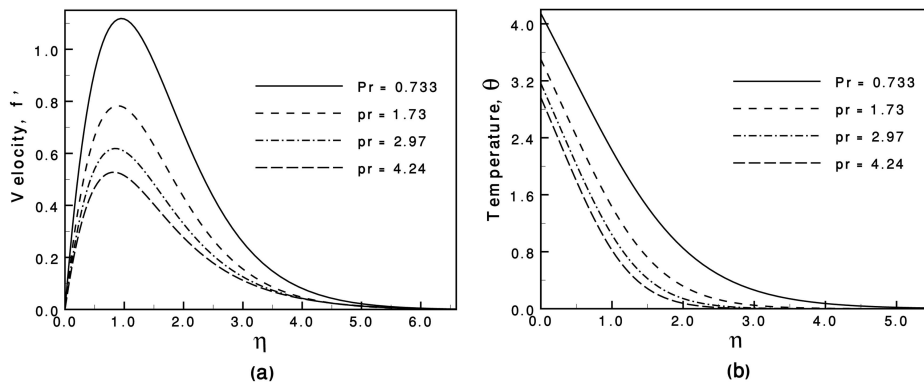


Fig. 4. (a) Variation of velocity profiles and (b) variation of temperature profiles against η for varying of Pr with $M = 0.10$, $n = 0.01$ and $p = 0.25$.

The effect of conjugate conduction parameter p for $M = 0.10$, $n = 0.01$ and $Pr = 0.733$ on the velocity and temperature profiles are shown in Fig. 5(a) and Fig. 5(b), respectively. From Fig. 5(a) it can be noted that the velocity is retarded and the peak velocity moves away from the interface for the higher values of p . From Fig. 5(b), it can be seen that the temperature of the fluid within the boundary layer decreases for the increasing p . A lower wall conductance κ_s or higher convective cooling effect due to greater κ_∞ and Gr increases the value of p as well as causes greater temperature difference between the two surfaces of the plate. The temperature at the solid-fluid interface is reduced since the temperature at the outside surface of the plate is kept constant. As a result the temperature profile shifts downwards in the fluid and eventually the velocity of the fluid within the boundary layer decreases.

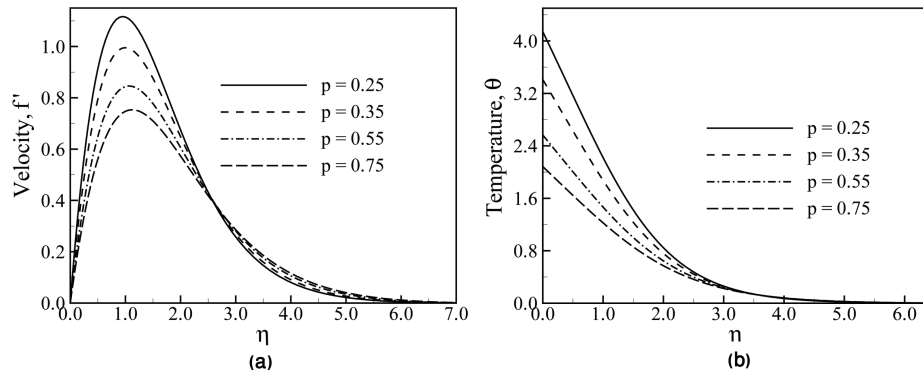


Fig. 5. (a) Variation of velocity profiles and (b) variation of temperature profiles against η for varying of p with $M = 0.10$, $n = 0.01$ and $Pr = 0.733$.

The variation of the local skin friction coefficient C_{fx} and surface temperature $\theta(x, 0)$ for different values of M with $Pr = 0.733$, $n = 0.01$ and $p = 0.25$ at different positions of x are illustrated in Fig. 6(a) and Fig. 6(b), respectively. It is observed from Fig. 6(a) that the increase value of the Magnetic parameter M leads to a decrease in the skin friction factor. Again Fig. 6(b) shows that the surface temperature $\theta(x, 0)$ increases due to the increased value of the magnetic parameter M . It can also be seen that the surface temperature increases in a certain region and then decreases along the upward direction of the plate for a particular M . The magnetic field acting against the flow reduces the skin friction and produces the temperature at the interface.

Fig. 7(a) and Fig. 7(b) illustrate the effect of the thermal conductivity variation parameter on the skin friction coefficient and surface temperature distribution against x with $M = 0.10$, $Pr = 0.733$ and $p = 0.25$. From Fig. 7(a) it is seen that the skin friction coefficient increases monotonically along the upward direction of the plate for a particular value of n . It is also seen that the skin friction factor increases for the increasing n . From Fig. 7(b) it is seen that the surface temperature increases for the increasing n . This is to be expected because the higher value of the thermal conductivity variation parameter accelerates the fluid flow and increases the temperature as mentioned in Fig. 3(a) and 3(b),

respectively.

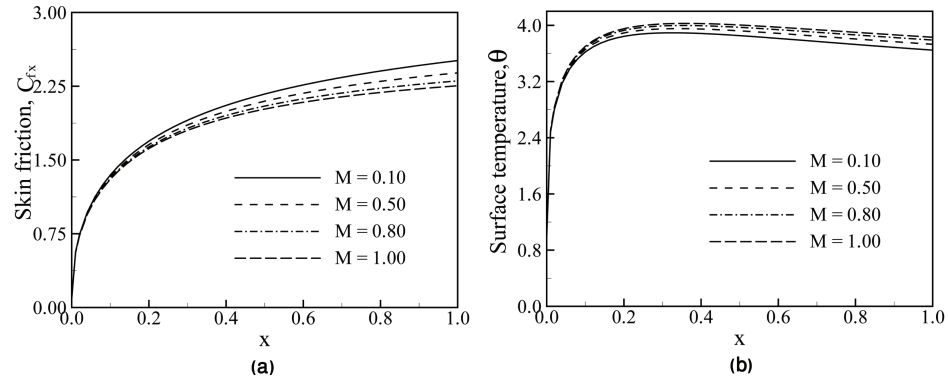


Fig. 6. (a) Variation of skin friction coefficients and (b) variation of surface temperature distributions against x for varying of M with $n = 0.01$, $Pr = 0.733$ and $p = 0.25$.

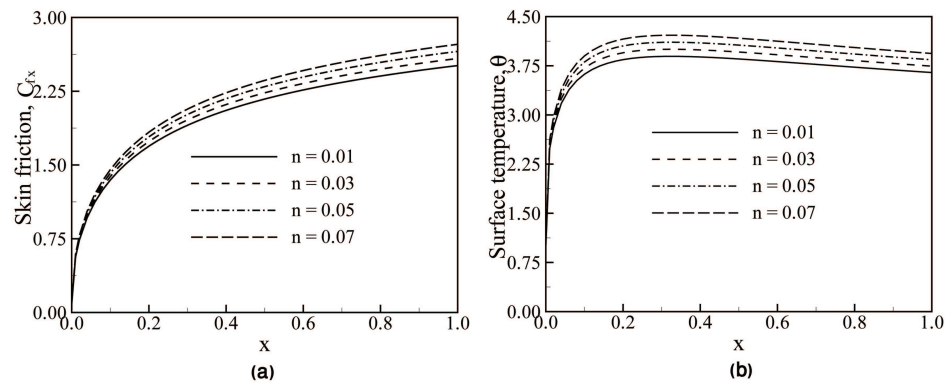


Fig. 7. (a) Variation of skin friction coefficients and (b) variation of surface temperature distributions against x for varying of n with $M = 0.10$, $Pr = 0.733$ and $p = 0.25$.

Fig. 8(a) and Fig. 8(b) deal with the effect of Prandtl number on the skin friction coefficient and surface temperature distribution against x with $M = 0.10$, $n = 0.01$ and $p = 0.25$. It can be observed from Fig. 8(a) that the skin friction coefficient increases monotonically for a particular value of Pr . It can also be noted that the skin friction coefficient decreases for the increasing Pr . From Fig. 8(b), it can be seen that the surface temperature distributions decrease owing to the increase of the Prandtl number. Moreover, the surface temperature increases in a certain region and then decreases along the positive x -direction for a particular Pr .

Fig. 9(a) and Fig. 9(b) deal with the effect of the conjugate conduction parameter on the local skin friction factor and the surface temperature with $M = 0.10$, $n = 0.01$ and $Pr = 0.733$. From Fig. 9(a) it is observed that the skin friction decreases for the

increasing p . Moreover, the skin friction co-efficient increases for a particular value of p along the upward direction of the plate. Again from Fig. 9(b) it is seen that the surface temperature decreases for the increasing p . Furthermore, the surface temperature increases in a certain region and then decreases along the positive x -direction. This is because the higher value of p reduces the fluid flow and decreases the temperature as mentioned in Fig. 5(a) and Fig. 5(b), respectively.

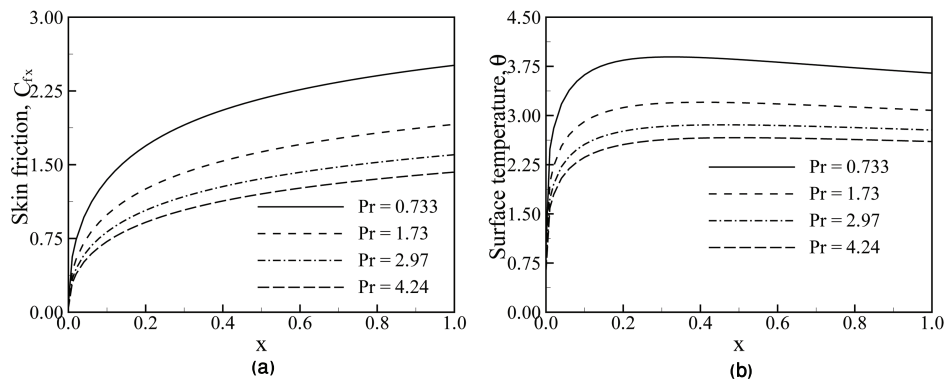


Fig. 8. (a) Variation of skin friction coefficients and (b) variation of surface temperature distributions against x for varying of Pr with $M = 0.10$, $n = 0.01$ and $p = 0.25$.

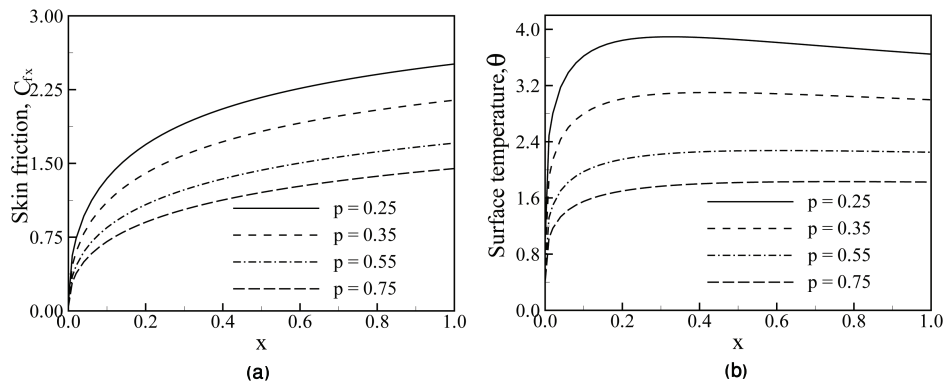


Fig. 9. (a) Variation of skin friction coefficients and (b) variation of surface temperature distributions against x for varying of p with $M = 0.10$, $n = 0.01$ and $Pr = 0.733$.

4 Conclusion

The effect of thermal conductivity variation due to temperature on MHD free convection flow along a vertical flat plate with wall conduction resistance has been studied. Numerical results of the equations governing the flow are obtained by using implicit finite

difference method together with Keller-box technique. An increase in the values of the thermal conductivity variation parameter n , magnetic parameter M leads to an increase in the surface temperature. Moreover, the surface temperature decreases for the increasing Pr and conjugate conduction parameter p . The velocity within the boundary layer increases for decreasing M , Pr and p and increasing n . On the other hand, the temperature within the boundary layer increases for the increasing M and n and decreasing Pr and p . Moreover, the skin friction coefficient decreases for the increasing M , Pr and p and decreasing n .

References

1. Cheng Long Chang, A numerical simulation of micro polar fluid flow along a flat plate with wall conduction and buoyancy effects, *J. Appl. Phys. D*, **39**, pp. 1132–1140, 2006.
2. J. H. Merkin, I. Pop, Conjugate free convection on a vertical surface, *Int. J. Heat Mass Tran.*, **39**, pp. 1527–1534, 1996.
3. A. Pozzi, M. Lupo, The coupling of conduction with laminar natural convection along a flat plate, *Int. J. Heat Mass Tran.*, **31**, pp. 1807–1814, 1988.
4. M. Miyamoto, J. Sumikawa, T. Akiyoshi, T. Nakamura, Effects of axial heat conduction in a vertical flat plate on free convection heat transfer, *Int. J. Heat Mass Tran.*, **23**, pp. 1545–1553, 1980.
5. I. Pop, D. Lesnic, D. B. Ingham, The conjugate mixed convection on a vertical surface in a porous medium, *Int. J. Heat Mass Tran.*, **38**, pp. 1517–1525, 1995.
6. H. T. Chen, S. M. Chang, The thermal interaction between laminar film condensation and forced convection along a conducting wall, *Acta Mech.*, **118**, pp. 13–26, 1996.
7. J. J. Shu, I. Pop, The thermal interaction between free convection and forced convection along a vertical conducting wall, *Int. J. Heat Mass Tran.*, **35**, pp. 33–38, 1999.
8. M. A. Hossain, The viscous and Joule heating effects on MHD free convection flow with variable plate temperature, *Int. J. Heat Mass Tran.*, **35**(12), pp. 3485–3487, 1992.
9. H. B. Keller, Numerical methods in the boundary layer theory, *Annu. Rev. Fluid Mech.*, **10**, pp. 417–433, 1978.
10. Md. M. Molla, A. Rahman, L. T. Rahman, Natural convection flow from an isothermal sphere with temperature dependent thermal conductivity, *J. Archit. Marine Eng.*, **2**, pp. 53–64, 2005.
11. T. Cebeci, P. Bradshaw, *Physical and Computational Aspects of Convective Heat Transfer*, Springer, New York, 1984.
12. J. Charraudeau, Influence de gradients de propriétés physiques en convection force application au cas du tube, *Int. J. Heat Mass Tran.*, **18**, pp. 87–95, 1975.
13. A. K. Luikov, Conjugate convective heat transfer problems, *Int. J. Heat Mass Tran.*, **16**, pp. 257–265, 1974.

14. J. H. Merkin, I. Pop, Conjugate free convection on a vertical surface, *Int. J. Heat Mass Tran.*, **39**, pp. 1527–1534, 1996.
15. I. Pop, D. B. Ingham, *Convective Heat Transfer*, Pergamon, Oxford, 2001.